Adsorption (2007) 13: 215–223
DOI 10.1007/s10450-007-9048-y

The options of interference microscopy to explore the significance of intracrystalline diffusion and surface permeation for overall mass transfer on nanoporous materials

L. Heinke · P. Kortunov · D. Tzoulaki · J. Kärger

Received: 27 April 2007 / Revised: 30 July 2007 / Accepted: 11 September 2007 / Published online: 26 September 2007

Abstract After a short introduction into interference microscopy and its potentials in monitoring transient concentration profiles in nanoporous materials, we concentrate on the special options of an analysis of these profiles close to the crystal surfaces. We shall in particular introduce a novel route of correlating the overall uptake, at a certain instant of time, with the current boundary concentration. In this way, the significance of surface resistances to overall molecular uptake may be most vividly demonstrated. Considering a large variety of nanoporous host-guest systems, including methanol in zeolites ferrierite, methanol in MOF Manganese(II)-formate and methanol in SAPO STA-7, quite different patterns of surface resistivities may be observed. A generalized analysis is complicated by the fact that both the diffusivities and the surface permeabilities are found to notably depend on the actual concentration. As a consequence, for one and the same system and over identical pressure steps, the relative contributions of diffusion and surface permeation to the overall process may be quite different for desorption and adsorption.

Keywords Diffusion · Surface resistance · Interference microscopy

Abbreviations

α	surface permeability (m s^{-1})
c	relative concentration (change)
c_{surf}	relative concentration at the crystal edge
D	transport diffusivity (m^2 s^{-1})
l	half channel length (m)
L	parameter $\alpha \cdot l/D$
m	relative uptake by the crystal
τ_{diff}	time constant of mass transport only limited by diffusion (s)
τ_{surf}	time constant of mass transport only limited by surface resistance (s)
$\tau_{\text{surf+diff}}$	time constant of mass transport limited by diffusion and surface resistance (s)
w	intercept of the asymptote of the c_{surf}-m-correlation plot with the ordinate
x, y, z	space coordinates (m)

L. Heinke · P. Kortunov · D. Tzoulaki · J. Kärger (✉)
Faculty of Physics and Geosciences, University of Leipzig,
Linnéstr. 5, 04103 Leipzig, Germany
e-mail: kaerger@physik.uni-leipzig.de

P. Kortunov
Corporate Strategic Research, ExxonMobil Research and
Engineering Company, Annandale, New Jersey 08801, USA

1 Introduction

Interference microscopy (Schemmert et al. 1999) allows a direct monitoring of the evolution of the intracrystalline concentration profiles during transient sorption experiments. With a spatial resolution of down to the range of micrometers, interference microscopy has thus proved to be the first "microscopic" technique applicable to the study of molecular diffusion in nanoporous host-guest systems under non-equilibrium conditions. This peculiarity, in particular, opened up the option to monitor the evolution of concentration profiles during molecular uptake or release. As a most remarkable finding of the first measurements by this technique, for many host-guest systems under transient conditions the boundary concentration close to the particle surfaces was found to notably deviate from the equilibrium value corresponding to the pressure of the guest molecules in the surrounding atmosphere. These differences indicate the presence of transport resistances at the external surface

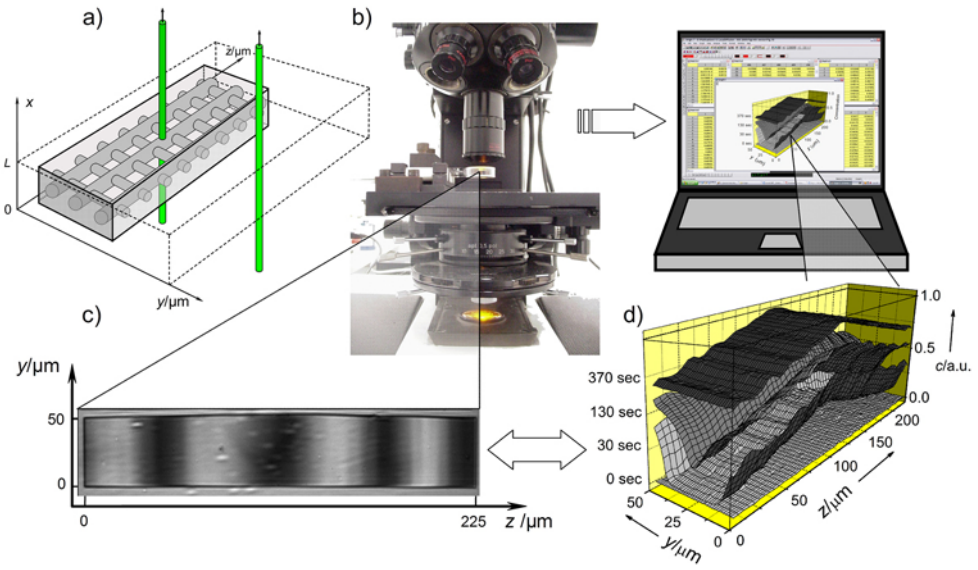

Fig. 1 Schematics of interference microscopy. (**a**) Two light beams; one passing through the crystal and the other through the surrounding atmosphere, (**b**) the interference microscope, (**c**) interference patterns generated due to different optical properties of the media passed by the two beams, (**d**) concentration profiles calculated from the changes in interference patterns with time

of the host systems, since any essential influence of heat release may be excluded (Heinke et al. in press), owing to the fact that the measurements are performed with single crystals ensuring sufficiently large surface-to-volume ratio (Lee and Ruthven 1979). The discussion of the relative contributions of diffusion and surface barriers on the overall kinetics of molecular uptake and release with nanoporous materials, accessible by interference microscopy, is in the focus of this contribution.

After an introduction to the principles of interference microscopy and its application to diffusion measurement in Sect. 2, Sect. 3 provides a survey of transient concentration profiles during molecular uptake and release for various host-guest systems. Their knowledge permits a representation of the boundary concentration as a function of the total amount adsorbed or released (rather than of the time elapsed as the usual way of representing data of sorption kinetics). The special features and potentials of this option are explored in Sect. 4. Finally, in Sect. 5, the experimental data presented in Sect. 3 are discussed on the basis of this formalism.

2 Fundamentals of interference microscopy and experimental procedure

The application of interference microscopy to diffusion studies with nanoporous (optically transparent) host materials is based on the fact that their optical density is a function of the nature and of the concentration of the guest molecules. In our studies, we use a JENAPOL interference microscope with an interferometer of Mach-Zehnder type where one observes the superposition of the crystal under study with its surroundings (Schemmert et al. 1999). Thus, changes in molecular concentration will correspondingly affect the interference pattern so that, in turn, changes in the interference patterns allow the determination of the changes in molecular concentration. Figure 1 provides a schematic illustration of this procedure. The quantity directly accessible is the integral $\int c(x, y, z)\mathrm{d}x$ where x is the coordinate in the observation direction of the microscope. The integral is to be taken over the whole crystal. For diffusion in only one or two direction(s) and observation perpendicular to these directions, the integral simply becomes the product of $c(x, y, z)$ and the crystal extension in x-direction where the concentration is only a function of y and z (for two-dimensional diffusion) or of only one coordinate for one-dimensional diffusion. In our studies, spatial and temporal resolution are on the order of $\Delta y \times \Delta z \approx 0.5\ \mu\mathrm{m} \times 0.5\ \mu\mathrm{m}$ and 10 s, respectively.

Figure 2 provides an impression of the experimental setup. Before being introduced into the glass cuvette for microscopic observation, the host system under study is activated following the specific procedure appropriate for the given material (in general by temperature increase at a rate of 60 $\mathrm{K\,h^{-1}}$ up to typically 200 °C under continued evacuation and by keeping the sample at the final temperature under continued evacuation for additional 10 h). Sufficiently large supply volumes and the tiny size of the crystal under study ensure the option of a true stepwise variation of the external pressure. All experiments were performed at room temperature with one selected crystal.

3 The considered concentration profiles

3.1 Methanol in zeolite ferrierite

The investigated silica ferrierite crystals are cation-free and have a dimension of about 10 µm × 50 µm × 200 µm. They have a shape of a cuboid body with a "roof" on both elongated sides (Fig. 3). They were synthesized at the University

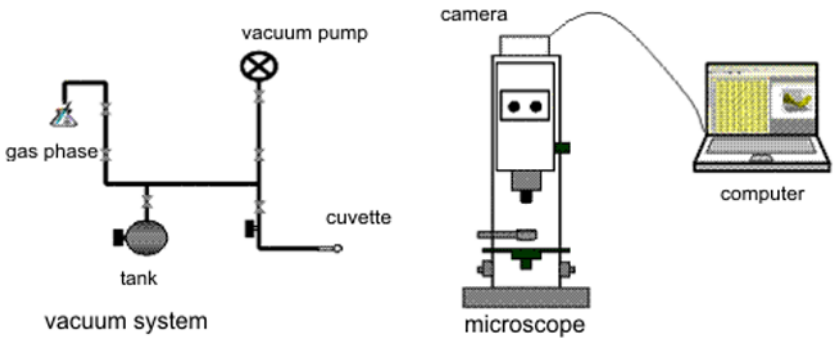

Fig. 2 Sketch of the experimental setup, with the vacuum system and the interference microscope

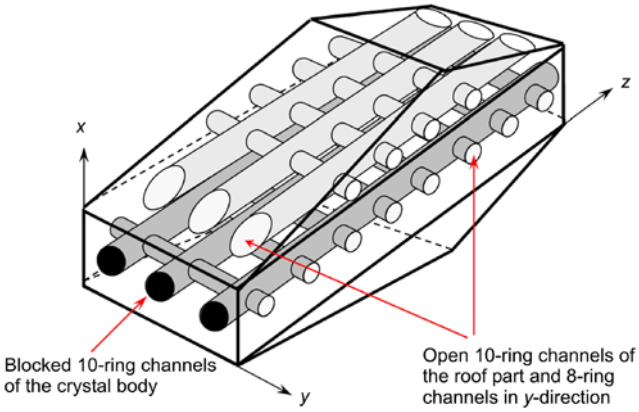

Fig. 3 Schematic representation of the ferrierite crystal with its two-dimensional pore structure. The figure shows partially blocked z-direction channels in the main body of the crystal, open z-direction channels in the roof section and open y-direction channels (Kärger et al. 2006)

of Stuttgart (Rakoczy et al. 2007) and they were activated under high vacuum at a temperature of 400 °C for 12 h. To ensure that there are no organic residues, the activation was preceded by exposing the sample to oxygen at 700 °C for 4 h.

The ferrierite crystals exhibit a two-dimensional channel structure with wider, "ten-membered" ring (formed by ten silica and ten oxygen atoms) channels along the z-direction with an elliptical cross section of 0.54 nm × 0.42 nm. There are smaller, "eight-membered" ring channels along the y-direction with an elliptical cross section of 0.48 nm × 0.35 nm. The smaller y-direction channels intersect the bigger channels and there are 12 such intersections per unit cell. Unless structural defects exist in the crystal lattice, there should be no transport in x-direction as there exist no channels in this direction. Based on the structure of the ferrierite crystal, one expects to find concentration gradients in y- and z-directions but none in x-direction (direction of the light beams).

As already shown in Kärger et al. (2006) the mass transport of methanol in the body of the ferrierite crystal is almost one-dimensional along the eight-ring channels in y-direction. Only small amounts of guest molecules enter the crystal along the ten-ring channels in z-direction in which, because of the bigger diameter, the diffusivity is very high and excludes measurable concentration gradients.

It is noteworthy that the concentrations at $y = 0$ and 50 µm do not immediately attain the equilibrium concentration. One has to conclude, therefore, that in addition to the very pronounced transport barriers at $z = 0$ and $z = 225$ µm, essentially precluding diffusion in z-direction, there are also transport resistances at the entrances of the eight-ring channels in y-direction. Figure 4 provides an overview of the evolution of the concentration profiles during methanol uptake by ferrierite following a pressure step from 0 to 10 mbar, 5 to 10 mbar and 0 to 80 mbar in the surrounding atmosphere for the adsorption process as well as from 10 to 5 mbar, 80 mbar to vacuum and 10 mbar to vacuum for the desorption process.

3.2 Methanol in MOF manganese formate

The MOF manganese formate investigated in these studies has been synthesized by M. Arnold and J. Caro at the University of Hannover (Arnold et al. 2007). Together with micrographs of the crystal under study, Fig. 5 provides a schematic view of the structure of the material indicating the one-dimensional channel structure. Prior to the uptake experiments, the samples were activated for 24 h at 150° under reduced pressure. Figure 6 shows the entity of concentration profiles in y-direction at $x = 41$ µm resulting from the evolution of the interference patterns during methanol uptake for a pressure step from 0 to 10 mbar in the surrounding atmosphere (Kortunov et al. 2007).

3.3 Methanol in zeolite SAPO STA-7

The zeolite SAPO STA-7 is of the new structure type SAV. The material used in our studies was synthesized by M.J. Castro and P.A. Wright at the University in St. Andrews, Scotland. In this crystal, there exists a three-dimensional channel system which consists of channels in z-direction with a diameter of 0.4 nm and channels in x- and

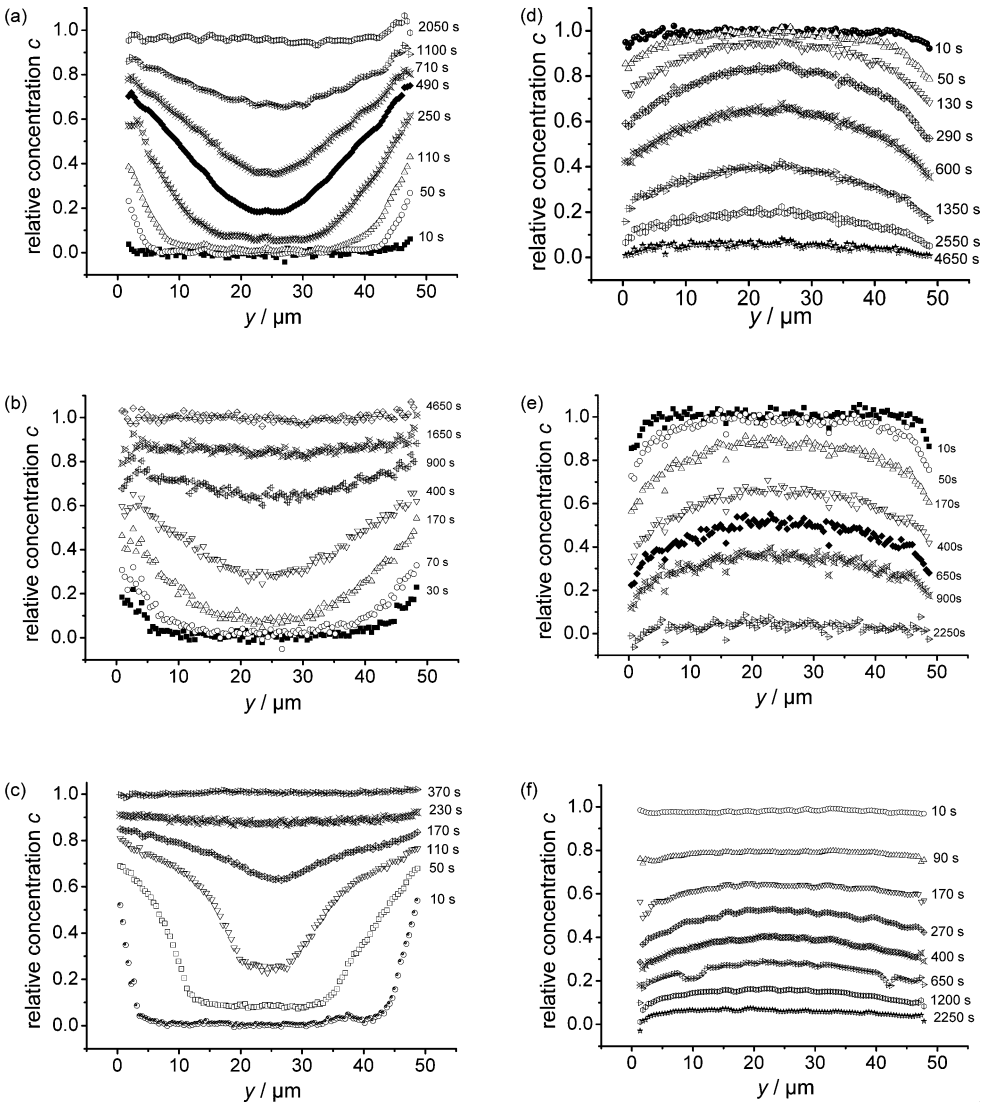

Fig. 4 Experimental concentration profiles in the y-direction of ferrierite type crystals for a pressure step of $0 \rightarrow 10$ mbar (**a**), $5 \rightarrow 10$ mbar (**b**), $0 \rightarrow 80$ mbar (**c**), 10 mbar $\rightarrow 0$ (**d**), $10 \rightarrow 5$ mbar (**e**) and 80 mbar $\rightarrow 0$ (**f**) of methanol in the surrounding atmosphere at selected times (Kortunov et al. 2006) of the total amount adsorbed (released)

y-direction with a diameter of 0.37 nm each (Fig. 7). The edge lengths of the (cuboid-like) crystal used in these studies are about 38 µm in z- and about 30 µm in x- and y-direction. Before the experiment, the crystal was activated under vacuum at 200 °C for 10 h. Figure 8 provides an overview of the evolution of the concentration profiles during methanol uptake following a pressure step from 0 to 1 mbar in the surrounding atmosphere.

4 Correlating molecular uptake with the actual boundary concentrations

Relative molecular uptake (or release) up to a certain observation time follows by simple integration over the concentration profiles for the given instant of time. Thus, the representations summarized in Sect. 3 provide the option to plot the boundary concentration as a function of the molecular uptake. Before, in Sect. 5, we are going to subject our experimental data to this procedure, in the present context the thus attainable evidence shall be discussed on the basis of the available analytical solutions. In most of the systems considered in Sect. 3 (methanol in ferrierite or MOF), one-dimensional diffusion is the by far prevailing mechanism. Hence, in the analytical treatment we may restrict ourselves to one-dimensional diffusion. Confining to the initial stage of uptake and release, also for SAPO STA-7 diffusion proceeds essentially one-dimensionally, namely perpendicular to the crystal faces. Moreover, it may be shown (Heinke in preparation) that even by plotting the total uptake curves, essentially the same patterns as for one-dimensional diffusion result.

Assuming a constant diffusivity D and a constant surface permeability α, the normalized concentration profile within

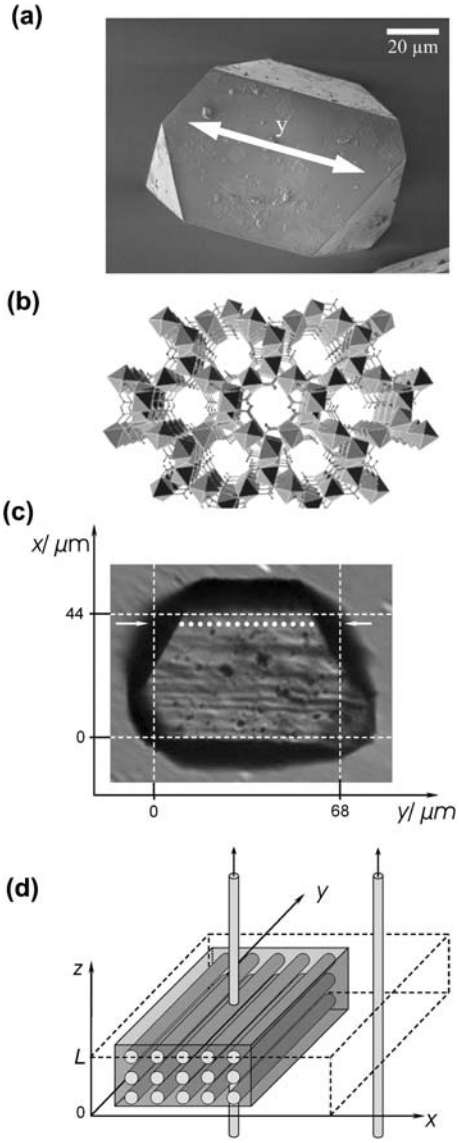

Fig. 5 SEM image of a typical ($Mn(HCO_2)_2$) crystal with indicated y-axis (**a**), scheme of the one-dimensional channel structure of ($Mn(HCO_2)_2$) along y-axis (**b**), crystal part (white dots at $x = 41$ µm) in which the profiles shown in Fig. 6b have been measured (**c**), and simplified one-dimensional pore structure of ($Mn(HCO_2)_2$) and the measuring principle based on the observation of the interference pattern between the light beams passing the crystal and the surrounding atmosphere (**d**) (Kortunov et al. 2007)

a host particle of length $2l$ during molecular uptake is given by the relation (Crank 1975)

$$c(y,t) = 1 - \sum_{n=1}^{\infty} \frac{2L\cos(\beta_n y/l)\exp(-\beta_n^2 Dt/l^2)}{(\beta_n^2 + L^2 + L)\cos\beta_n} \tag{1}$$

where the β_n′s are the positive roots of

$$L = \frac{l\alpha}{D} = \beta_n \tan\beta_n. \tag{2}$$

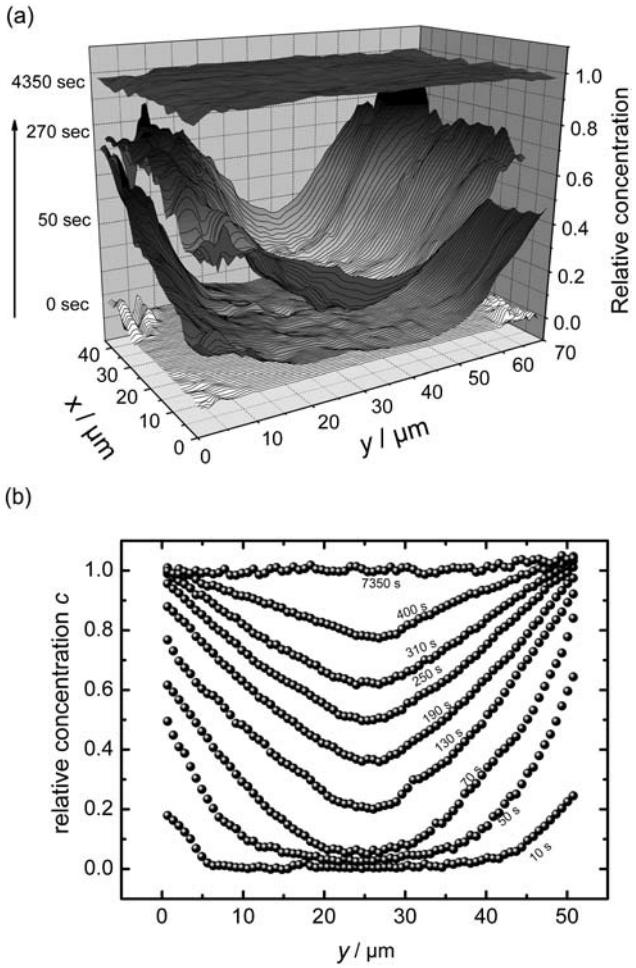

Fig. 6 Evolution of two-dimensional concentration profiles (**a**) and one-dimensional concentration profiles (**b**) in y-direction (near the edge, $x = 41$ µm) of methanol in a MOF crystal for a pressure step of $0 \rightarrow 10$ mbar at selected times

Integration over the system in diffusion (i.e. y-) direction from $-l$ to l yields

$$m(t) = 1 - \sum_{n=1}^{\infty} \frac{2L^2\exp(-\beta_n^2 Dt/l^2)}{(\beta_n^2 + L^2 + L)\beta_n^2} \tag{3}$$

for the relative uptake at time t. The implied constancy of D and α effects that (1) and (3) hold for uptake from concentration zero as well as for any subsequent step, where then (1) denotes the change in concentration rather than the concentration itself. Equivalently, the corresponding expressions for molecular release are just the sums in (1) and (3). This may be easily rationalized by realizing that, as a consequence of the implied constancy of D and α, the underlying diffusion equation is linear. Hence, the simultaneous occurrence of adsorption and desorption has to leave the system unchanged.

Figure 9 displays the correlation between the actual boundary concentration (c_{surf}) and the relative uptake (m)

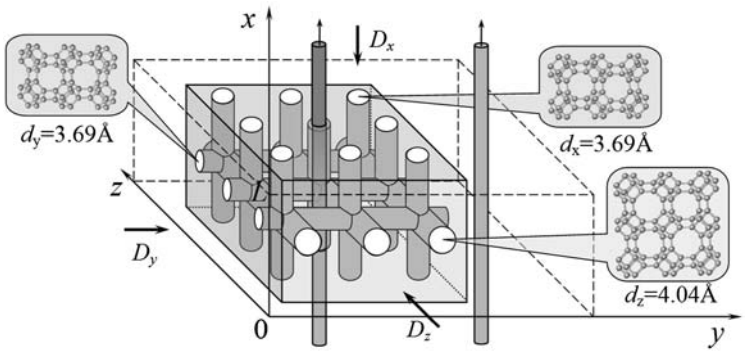

Fig. 7 SAPO STA-7 crystal with the three-dimensional pore structure. The channel cross sections of each channel are also shown

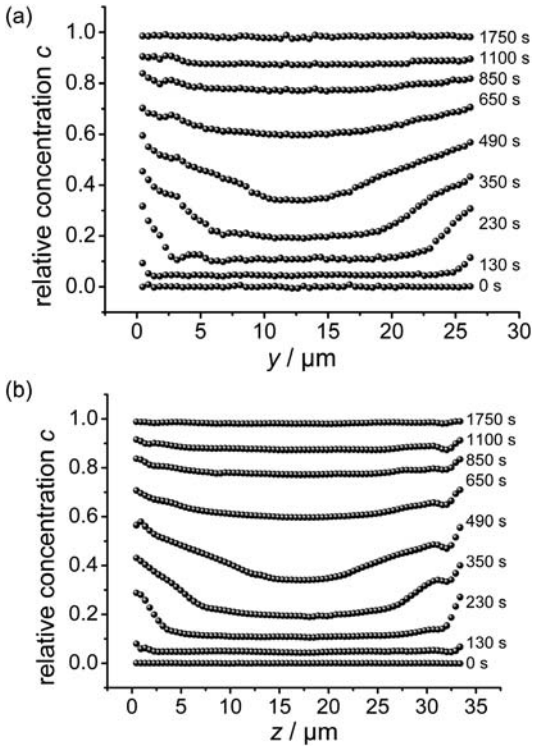

Fig. 8 Concentration profiles measured with IFM (viz. integrated concentration $\int_0^{2l_x} c(x, y, z)\mathrm{d}x$) along y-direction (**a**) and z-direction (**b**) in the centre of the crystal, this means $z = 19$ µm (**a**) and $y = 15$ µm, respectively

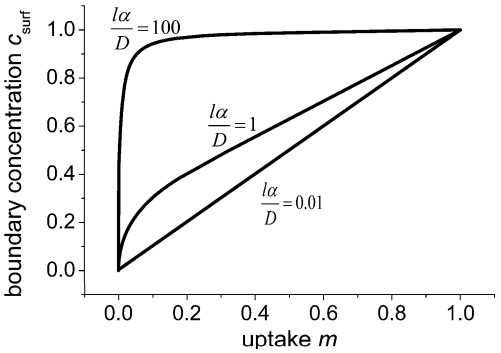

Fig. 9 Correlation between the actual boundary concentration (c_{surf}) and the relative uptake (m) at the corresponding instant of time. Three different cases are shown: the mass transport is essentially limited by intracrystalline diffusion ($l\alpha/D = 100$), by surface barriers ($l\alpha/D = 0.01$) and both by intracrystalline diffusion and surface resistance ($l\alpha/D = 1$)

at the corresponding instant of time, following from (1) for $y = -l$ or l and (3). The ratio $l\alpha/D$ has been chosen as the parameter of this representation. It represents nothing else than the ratio $\tau_{\mathrm{diff}}/\tau_{\mathrm{surf}}$ of the exchange times ("first moments" of the tracer-exchange, sorption or desorption curves which, owing the implied constancy of D and α, have to coincide). Thus, it turns out that with increasing uptake the correlation plot very soon becomes a straight line. Its intercept with the ordinate (in the following referred to as w) varies strongly with the prevailing mechanism of transport resistance. For dominating surface barriers (e.g. for $\frac{4}{\pi^2}\frac{l\alpha}{D} = \frac{\tau_{diff}}{\tau_{surf}} = 10^{-2}$), the total plot appears as a straight line with no perceptible intercept with the ordinate. With increasing influence of diffusion, this intercept becomes more and more extended.

In the long-time limit (only considering the first summand), (3) may be easily combined with (1) at $y = -l$ or l yielding

$$c_{surf}(t) = c(y = l, t) = 1 - \frac{\beta_1^2}{L} + \frac{\beta_1^2}{L} \cdot m(t). \tag{4}$$

Thus, the intercept w of the asymptote of the c_{surf}-m-correlation plot to the ordinate is found to be given by the relation

$$w = 1 - \frac{\beta_1^2}{L}. \tag{5}$$

In a qualitative way, from the representations of Fig. 9, the reciprocal value of this intercept, w^{-1}, is expected to indicate the relevance of surface barriers for the overall process of molecular exchange. The ratio of the quotient of the exchange times and the reciprocal value of w can be reformulated to

$$\frac{\tau_{\mathrm{surf+diff}}/\tau_{\mathrm{diff}}}{w^{-1}} = \frac{\pi^2}{4}\left(\frac{1 - \beta_1/\tan\beta_1}{\beta_1^2}\right) \tag{6}$$

which results to be between $\pi^2/12 \approx 0.82$ and 1 for β_1 varying in the range of 0 and $\pi/2$ (corresponding to a variation of $L = \frac{l\alpha}{D} = \beta_1 \tan\beta_1$ between 0 and ∞, i.e. over all possible values). Therefore, the reciprocal value of the intercept of the extrapolated linear part of the c_{surf}-m-correlation plot with the ordinate may be taken as an estimate of the factor, by which the presence of the surface barrier leads to a prolongation of molecular uptake and release.

The equivalence of the ratio of the exchange times $\tau_{surf+diff}/\tau_{diff}$ and the reciprocal value of the intercept w^{-1} (6) implies concentration-independent transport parameters. In real systems, however, the transport diffusivity, as well as the surface permeability, may depend on concentration. However, as shown in (Heinke in preparation) with a huge variety of different concentration dependencies for the transport diffusivity and surface permeability, the reciprocal intercept w^{-1} may quite generally be taken as an excellent estimate of the ratio $\tau_{surf+diff}/\tau_{diff}$.

5 Discussion of the measured concentration profiles

Figures 10, 11 and 12 provide a survey of the c_{surf}-m-correlation plots following from the transient concentration profiles shown in Figs. 4, 6 and 8. A summary of the resulting intercepts and the ratios $\tau_{surf+diff}/\tau_{diff}$ resulting with $\tau_{surf+diff}/\tau_{diff}/w^{-1} \approx 1$ are presented by Table 1.

The factor $\tau_{surf+diff}/\tau_{diff}$ by which the uptake or release is prolongated by the surface resistance depends, apart from the host-guest system, on the applied pressure step since the transport parameters vary with concentration. During the adsorption of methanol on ferrierite for a pressure step from 0 to 80 mbar, the uptake process is slowed down by the surface resistance by only a factor of less than 2 ($w = 0.55$, Fig. 10c) whereas, by the reduced surface permeability, the corresponding process of desorption is prolongated by a factor of approximately 10 ($w = 0.9$, Fig. 10f). The different behaviour of these two opposing transport processes

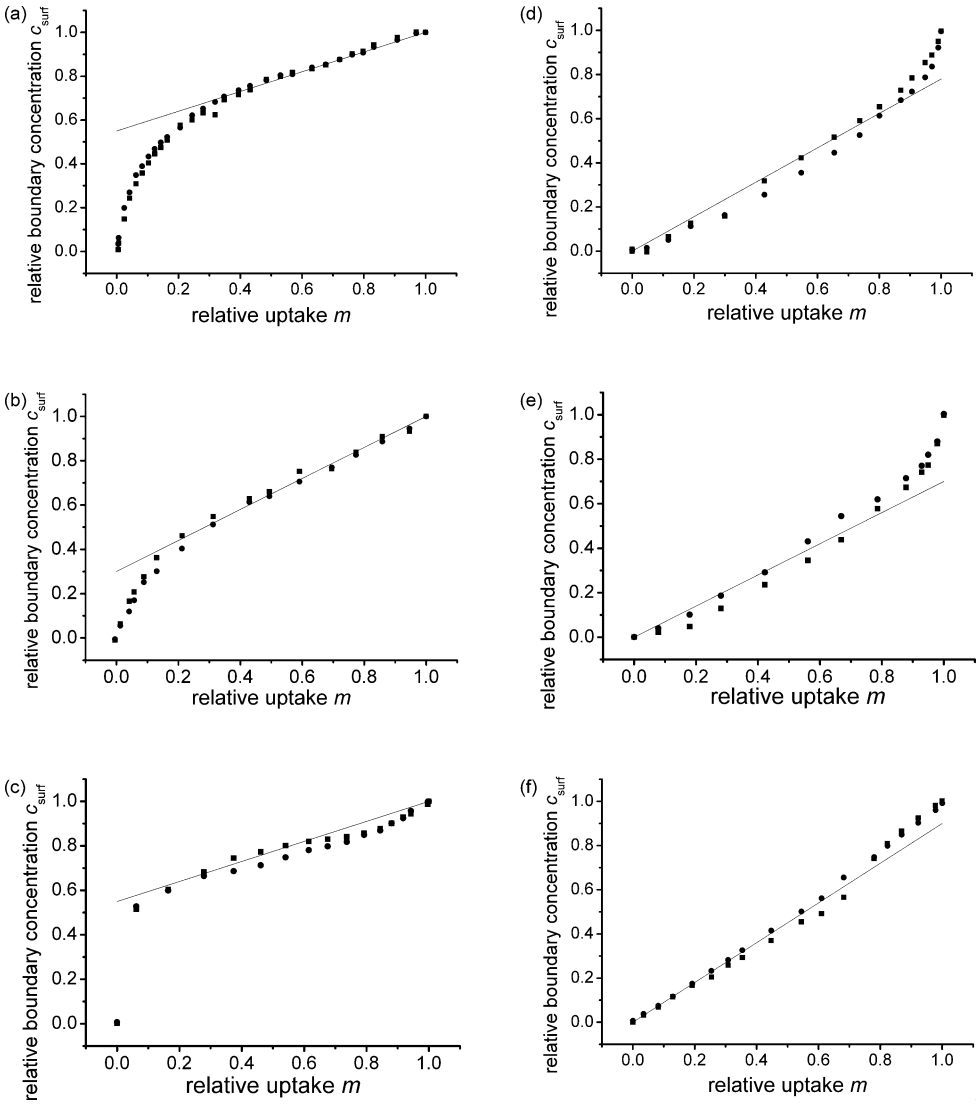

Fig. 10 Correlation between the actual boundary concentration (c_{surf}) and the relative uptake (m) at the corresponding instants of time for the uptake and release of methanol by ferrierite. The applied pressure steps are from 0 to 10 mbar (**a**), 5 to 10 mbar (**b**) and 0 to 80 mbar (**c**) as well as 10 mbar to 0 (**d**), 10 to 5 mbar (**e**) and 80 mbar to 0 (**f**)

Table 1

System	Pressure step	Interception w	$\tau_{surf+diff}/\tau_{diff}$
Methanol in ferrierite	$0 \rightarrow 10$ mbar	0.55	1.8
Methanol in ferrierite	$5 \rightarrow 10$ mbar	0.3	3.3
Methanol in ferrierite	$0 \rightarrow 80$ mbar	0.55	1.8
Methanol in ferrierite	10 mbar $\rightarrow 0$	$0.78 = 1 - 0.22$ (Des)	4.5
Methanol in ferrierite	$10 \rightarrow 5$ mbar	$0.7 = 1 - 0.3$ (Des)	3.3
Methanol in ferrierite	80 mbar $\rightarrow 0$	$0.9 = 1 - 0.1$ (Des)	10
Methanol in MOF	$0 \rightarrow 10$ mbar	0.65	1.5
Methanol in SAPO STA-7	$0 \rightarrow 1$ mbar	0.22	4.5
Methanol in SAPO STA-7	$0 \rightarrow 1$ mbar	0.22	4.5

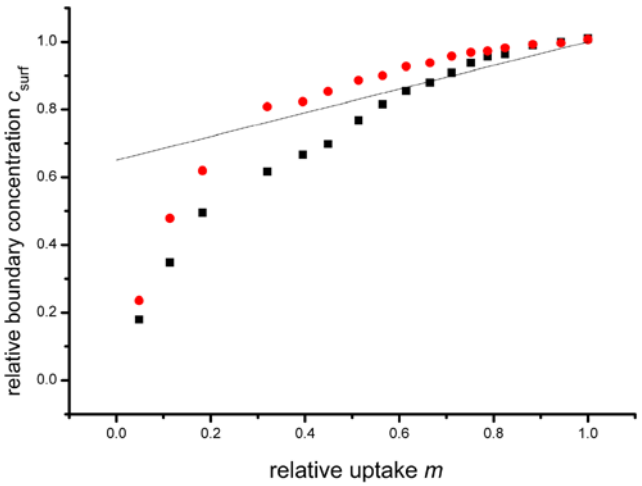

Fig. 11 Correlation between the actual boundary concentration (c_{surf}) and the relative uptake (m) at the corresponding instants of time for the uptake of methanol by MOF manganese formate for a pressure step from 0 to 10 mbar

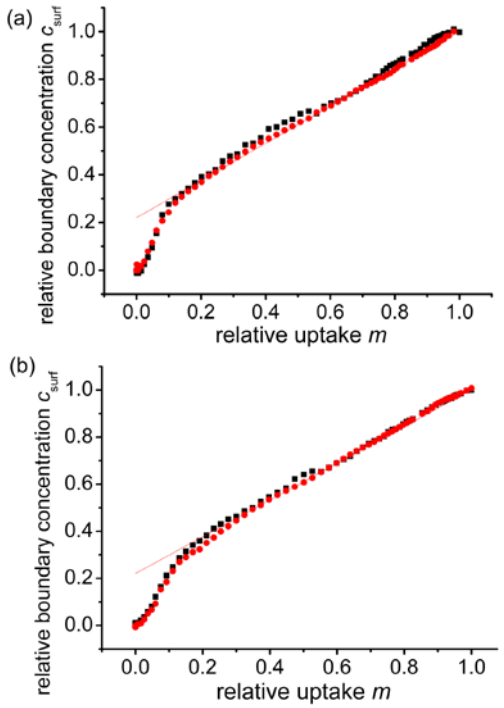

Fig. 12 Correlation between the boundary concentration integrated over x (c_{surf}) and the relative uptake (m) at the corresponding instants of time for the uptake of methanol by SAPO STA-7 for a pressure step from 0 to 1 mbar. The analysed direction is along y (**a**) and z (**b**)

is also visible from the intracrystalline concentration profiles. During the adsorption process the concentration profiles are curved which indicates a transport process limited by intracrystalline diffusion whereas during the corresponding desorption process the concentration profiles are flat. This indicates that the surface resistance restricts the overall transport process.

This opposing behaviour originates in the concentration dependence of the transport parameters. In the considered concentration range, the diffusivity of methanol in ferrierite increases by about two orders of magnitude (Kärger et al. 2006) whereas the surface permeability changes by only a small factor. Therefore, at high loadings the intracrystalline diffusion is very fast and the transport process is limited by the surface resistance whereas at low loadings the small diffusivity limits the transport process. This causes the contrary behaviour of adsorption and desorption at large pressures.

For the small pressure step from 5 to 10 mbar, adsorption and desorption of methanol in ferrierite can be described very well with constant transport parameters, namely $D = 8.1 \times 10^{-13}$ m^2 s^{-1} and $\alpha = 4.2 \times 10^{-8}$ m s^{-1} (Kortunov et al. 2005). This results in $l\alpha/D = 1.24$. The intercept w of the asymptote of the c_{surf}-m-correlation plot to the ordinate is found to be 0.3 for adsorption and desorption (Figs. 10b and 10e). With (2) and (5), this value of w leads to a ratio $l\alpha/D = 1.21$ which is in good agreement with the value determined by microscopic analysis.

In Fig. 11 w is estimated to 0.65. This indicates that mass transport of methanol in MOF manganese formate is mainly controlled by intracrystalline diffusion, with a prolongation of mass transfer by roughly 50% due to the sur-

face barrier. The ratio $l\alpha/D$ is herewith calculated to be 4.9. Microscopic analysis (Kortunov et al. 2007) reveals a constant transport diffusivity ($D = 1.5 \times 10^{-12}$ m^2 s^{-1}) and a surface permeability increasing with increasing concentration. Using the mean surface permeability ($\bar{\alpha} = \int_0^1 \alpha(c)\mathrm{d}c = 5.3 \times 10^{-7}$ m s^1), $l\bar{\alpha}/D$ follows to be 5.3. This is again in very good agreement with the value determined from the c_{surf}-m-correlation plots.

For methanol uptake by SAPO STA-7 the intersection is determined to 0.22 for both the y- and z-directions (Fig. 12). One has to conclude that here the uptake rate is significantly impaired by existence of the surface resistances which prolongate the time by a factor of approximately 4.5.

6 Conclusion

Application of interference microscopy to monitoring transient sorption on nanoporous host guest systems provides the option of a direct measurement of the evolving actual boundary concentration (c_{surf}), simultaneously with the total uptake (or release, m) of guest molecules up to this instant of time. In this way, for the first time the generation of "c_{surf}-m-correlation plots" has become possible. Following a short theoretical analysis of the options which, for constant diffusivities and surface permeabilities, may be deduced from such representations, for a number of host-guest systems (methanol in zeolite ferrierite, MOF manganese formate and zeolite SAPO STA-7) experimentally determined correlation plots are presented. It is in particular observed that, as a consequence of the dependence of the diffusivities and surface permeabilities on the loading, the correlation plots determined for adsorption and desorption may notably differ from each other. This finding reflects that, as a consequence of this concentration dependence, for one and the same pressure step, performed in forward and backward direction, i.e. during adsorption and desorption, respectively, the relative influence of the transport resistances by diffusion and surface permeation may be different. It is shown that these differences may be directly correlated with the influence of the respective concentration dependences. Thus, the c_{surf}-m-correlation plots turn out to be an attractive and productive novel tool for analysing and interpreting transient adsorption-desorption curves.

Acknowledgements We are obliged to Jens Weitkamp, Jürgen Caro and Paul Wright for supplying us with the nanoporous host materials applied in these studies and to Stefano Brandani, Christian Chmelik, Douglas M. Ruthven and D.B. Shaw for stimulating discussions. Financial support by Deutsche Forschungsgemeinschaft and Fonds der Chemischen Industrie is gratefully acknowledged.

References

Arnold, M., Kortunov, P., Jones, D.J., Nedellec, Y., Kärger, J., Caro, J.: Oriented crystallisation on supports and anisotropic mass transport of the metal-organic framework manganese formate. Eur. J. Inorg. Chem. **2007**, 60–64 (2007)

Crank, J.: The Mathematics of Diffusion, p. 266. Oxford (1975)

Heinke, L.: Significance of concentration-dependent surface permeation and intracrystalline diffusion for overall mass transfer. Diffus. Fundam. **4**, 12.1–12.11 (2007)

Heinke, L., Chmelik, C., Kortunov, P., Shah, D.B., Brandani, S., Ruthven, D.M., Kärger, J.: Analysis of thermal effects in infrared and interference microscopy: n-butane-5A and methanol-ferrierite systems. Microporous Mesoporous Mater. **104**, 18–25 (2007)

Kärger, J., Kortunov, P., Vasenkov, S., Heinke, L., Shah, D.B., Rakoczy, R.A., Traa, Y., Weitkamp, J.: Unprecedented insight into diffusion by monitoring the concentration of guest molecules in nanoporous host materials. Angew. Chem. Int. Ed. **45**, 7846–7849 (2006)

Kortunov, P., Chmelik, C., Kärger, J., Rakoczy, R.A., Ruthven, D.M., Traa, Y., Vasenkov, S., Weitkamp, J.: Sorption kinetics and intracrystalline diffusion of methanol in ferrierite: an example of disguised kinetics. Adsorption **11**, 235–244 (2005)

Kortunov, P., Heinke, L., Vasenkov, S., Chmelik, C., Shah, D.B., Kärger, J., Rakoczy, R.A., Traa, Y., Weitkamp, J.: Internal concentration gradients of guest molecules in nanoporous host materials: measurement and microscopic analysis. J. Phys. Chem. B **110**, 23821–23828 (2006)

Kortunov, P., Heinke, L., Arnold, M., Nedellec, Y., Jones, D.J., Caro, J., Kärger, J.: Intracrystalline diffusivities and surface permeabilities deduced from transient concentration profiles: methanol in MOF manganese formate. J. Am. Chem. Soc. **129**, 8041–8047 (2007)

Lee, L.K., Ruthven, D.M.: Analysis of thermal effects in adsorption rate measurements. J. Chem. Soc. Faraday Trans I **75**, 2406–2422 (1979)

Rakoczy, R.A., Traa, Y., Kortunov, P., Vasenkov, S., Kärger, J., Weitkamp, J.: Synthesis of large crystals of all-silica zeolite ferrierite. Microporous Mesoporous Mater. **104**, 179–184 (2007)

Schemmert, U., Kärger, J., Krause, C., Rakoczy, R.A., Weitkamp, J.: Monitoring the evolution of intracrystalline concentration. Europhys. Lett. **46**, 204–210 (1999)